LEVEL II

AD A098372

DTIC FILE COPY

OFFICE OF NAVAL RESEARCH

Contract N00014-79-0622

Task No. NR 056-729

TECHNICAL REPORT NO. 1

Production and Electron Diffraction Studies of Silver Metal Clusters in the Gas Phase

by

B. G. DeBoer and G. D. Stein

Prepared for Publication

in

Surface Science, in press (1981)

Northwestern University
Departments of Mechanical and Nuclear Engineering, Chemistry, and Physics
Evanston, Illinois 60201

April, 1981

(9) Technical rept.

SECURITY CLASSIFICATION OF THIS PAGE (When Data Entered)

REPORT DOCUMENTATION PAGE	READ INSTRUCTIONS BEFORE COMPLETING FORM
1. REPORT NUMBER: Technical Report No. 1	2. GOVT ACCESSION NO.: AD-A098 372
3. RECIPIENT'S CATALOG NUMBER	
4. TITLE (and Subtitle): Production and Electron Diffraction Studies of Silver Metal Clusters in the Gas Phase	5. TYPE OF REPORT & PERIOD COVERED: Interim
	6. PERFORMING ORG. REPORT NUMBER
7. AUTHOR(s): G. DeBoer and G. D. Stein	8. CONTRACT OR GRANT NUMBER(s): N00014-79-0622
9. PERFORMING ORGANIZATION NAME AND ADDRESS: Northwestern University, Departments of Mechanical and Nuclear Engineering, Chemistry, and Physics Evanston, Illinois 60201	10. PROGRAM ELEMENT, PROJECT, TASK AREA & WORK UNIT NUMBERS: NR 056-729
11. CONTROLLING OFFICE NAME AND ADDRESS: Office of Naval Research, Chemistry Program Code 472, Arlington, Virginia 22217	12. REPORT DATE: April, 1981
	13. NUMBER OF PAGES: 19
14. MONITORING AGENCY NAME & ADDRESS (if different from Controlling Office): ONR, Chicago, 536 S. Clark Street, Chicago, Illinois 60605 (14) TR-1	15. SECURITY CLASS. (of this report): Unclassified
	15a. DECLASSIFICATION/DOWNGRADING SCHEDULE

16. DISTRIBUTION STATEMENT (of this Report)
Distribution of this document has been approved for public release and sale; its distribution is unlimited.
(15) N00014-79-C-0622

17. DISTRIBUTION STATEMENT (of the abstract entered in Block 20, if different from Report)

18. SUPPLEMENTARY NOTES
Prepared for publication in Surface Science, in press (1981).

19. KEY WORDS (Continue on reverse side if necessary and identify by block number)
Clusters, Nucleation, Electron diffraction, Molecular beam, Silver

20. ABSTRACT (Continue on reverse side if necessary and identify by block number)
Silver is evaporated into an inert gas flowing at pressures between 0.1 and 3 torr and nucleates to form clusters in a size range of 40 to 110 Å. This two-phase mixture flows through a two stage molecular beam into a modified electron microscope. Electron diffraction patterns are taken in the cluster beam and analyzed assuming the bulk, face centered cubic unit cell and using a thirteen-beam, multislice, multiple scattering program. Deviations from the bulk structure are seen and are larger for smaller cluster size. Several possible interpretations are discussed. The use of inert

DD FORM 1 JAN 73 1473 EDITION OF 1 NOV 65 IS OBSOLETE S/N 0102-014-6601 | SECURITY CLASSIFICATION OF THIS PAGE (When Data Entered)

11576

81 5 12 036

SECURITY CLASSIFICATION OF THIS PAGE(When Data Entered)

20. molecular gasses as carriers is found to greatly increase cluster production.

SECURITY CLASSIFICATION OF THIS PAGE(When Data Entered)

PRODUCTION AND ELECTRON DIFFRACTION STUDIES OF SILVER METAL CLUSTERS IN THE GAS PHASE

by

B.G. De Boer† and G.D. Stein*

Northwestern University
Gasdynamics Laboratory
Evanston, Illinois 60201

ABSTRACT

Silver is evaporated into an inert gas flowing at pressures between 0.1 and 3 torr and nucleates to form clusters in a size range of 40 to 110 Å. This two-phase mixture flows through a two stage molecular beam into a modified electron microscope. Electron diffraction patterns are taken in the cluster beam and analyzed assuming the bulk, face centered cubic unit cell and using a thirteen-beam, multislice, multiple scattering program. Deviations from the bulk structure are seen and are larger for smaller cluster size. Several possible interpretations are discussed. The use of inert molecular gasses as carriers is found to greatly increase cluster production.

* to whom correspondence should be addressed
† present address: GTE Products Corp. 60 Boston St., Salem, MA 01970

INTRODUCTION

The objective of this study was to obtain information on the structure of small clusters of metal atoms, prepared by evaporation into a low pressure inert gas, by analysis of their electron diffraction patterns. Potentially large effects of supporting substrates upon the clusters' structures were avoided by employing the quenching gas as a carrier to transport the clusters through a differentially pumped gasdynamic system (forming a "molecular" beam) into a high vacuum region where the electron diffraction pattern can be recorded[1]. A necessary subsidiary goal was to discover conditions which produce sufficiently dense metal cluster beams so that electron diffraction patterns can be observed.

EXPERIMENTAL

The metal cluster generator has been described previously[1] and is schematically illustrated in Fig. 1. This oven cluster source has been mounted in one port of the "diffraction chamber" of an Hitachi HU-11A/B, operated as an electron beam source (condenser lenses only used). The electron microscope has been modified with the addition of a coarse aperture just above the cluster source and additional pumping capacity of 1,000 l/sec. Electron diffraction patterns are recorded on glass photographic plates.

The metal vapor source used was a small helix, hand-wound from tungsten wire (0.38 mm diameter) into which one or more small ingots, formed from 99.999% silver, are inserted. The amount of silver in each charge is estimated to be in the range 0.1 - 0.25 g. The gas

inlet tubing was shortened so that it now discharges from behind the heater rather than between heater and N_1 as shown in Fig. 1. Pressures measured at various points, with gas flow on but oven power off, are recorded in Table I. Except for the lowest pressure with helium, which is outside the range of operating conditions actually used, the pressure ratios are low enough to cause "choked", sonic, constant mass flow rates through both N_1 and N_2. However, due to the pressure drop through the inlet gas tube, this flow is everywhere subsonic.
The flow transit time for a monatomic gas is calculated to be ca. 0.5 sec for the oven chamber. One-fifth to one-eighth of the carrier gas exits via N_2. A somewhat higher proportion of the metal clusters ought to pass through N_2 and the electron beam, because of their much greater "molecular" weight (4×10^4 to 2×10^6).

Diffraction patterns, if observed at all, are commonly visible for only 10 seconds, and never for more than about 90 seconds. We were clearly not operating the oven under steady-state conditions, although they were constant over the plate exposure time (a fraction of a second). The oven gas pressure and temperature, P_o and T_o, along with other experimental information, are summarized in Table II.

Exposed plates were developed in the usual manner and their degree of blackening quantified by scanning across a diameter of the diffraction pattern with a recording microdensitometer. Patterns from three plates

are presented in Fig. 2. Peak spacings (diffraction ring diameters), peak widths, and peak heights are all measured from these densitometer records. Calibration of spacings and minimum peak widths was obtained by tracing the patterns obtained from a commercial aluminum diffraction standard. Unit cell dimensions were derived from ring radii using the expression:

$$a = L\lambda \sqrt{h^2 + k^2 + l^2} \; / \; (r(1 - 3r^2/8L^2)) \qquad (1)$$

where $L\lambda$ is a "camera constant" determined from the aluminum standard, $\lambda = 0.053551$ Å for the 50 Kev electrons, and $L = 47.13$ cm. The term in $(r/L)^2$ is a small flat-plate correction. Cluster diameters, D, were estimated from peak widths using

$$D = L\lambda \; / \; \sqrt{w^2 - w_o^2} \qquad (2)$$

where w is the observed peak width and w_o is the "instrument broadening" taken to be the peak width found for the aluminum standard. Peak heights were taken to be proportional to the diffracted power in each peak and were corrected for the non-linear response of the plates. Estimated standard deviations were assigned to each intensity, σ_{obs}, and multiplied by the same correction factors. It should be emphasized that only diffraction patterns strong enough to be seen by eye on the phosphor screen were recorded.

RESULTS AND DISCUSSION

Source performance

In addition to varying gas pressures and filament temperatures, in search of optimum conditions for the production of high densities of small clusters, we also explored the effect of changing the carrier gas. Argon and helium show differences reflecting their differing atomic masses and collision cross sections[2, 3]. Past experience with nucleation studies indicates that a larger number of smaller clusters should result from a more rapid cooling of the hot metal vapor[1]. The chemically inert molecular gas, sulfur hexafluoride SF_6, with its many internal degrees of freedom, i.e., its much larger heat capacity per molecule, should be a more effective third body in the early stages of cluster formation. Since silver has a relatively small affinity for oxygen, CO_2 was also successfully used as a carrier gas.

Greatly increased production of silver clusters was observed using molecular gases. This occurred at substantially lower filament temperatures (i.e., lower vapor pressures) as indicated in Table II. Silver deposits on the oven liner were collected on microscope grids. Electron diffraction patterns from samples showed metallic silver only, with no evidence for chemical reaction with the molecular gasses.

An argument was made in an earlier paper[1] for a relationship between cluster size and the product of oven pressure, P_o, times the temperature of the evaporating metal sample, T_{om}. The earlier study used the same cluster generator and used one carrier gas (Ar) and several metals (In, Bi, and Pb), while this work is for one metal (Ag) and several carrier gases (Ar, He, CO_2, and SF_6). Both sets of observations are displayed in Fig. 3. All the results with the filament source are consistent, the heavier gases producing a given cluster size at lower P_oT_{om}.

Diffraction Analysis

From the diffraction patterns, one easily obtains crystalline unit cell dimensions and crystallite sizes from the diffracted rings' diameters and breadths, respectively. However, more detailed atomic scale information is contained in the relative intensities of the rings. This information may be extracted by matching the intensities calculated from a model to the observed intensities. However, the calculations leading from model to diffracted intensities are more complex in the case of electron scattering than for X-rays or neutrons because of multiple scattering or "dynamical" effects. These effects are large enough to cast doubt upon any such analysis based upon simpler kinematic (or the first-approximation, Blackman-formula[4]) calculations[5]. Accordingly, a computer program has been written which calculates the diffracted intensities in as accurate an approximation as the available resources would permit. This program calculates the intensities of "systematically-related" sets of (from 5 to 13) diffracted beams using a Sturkey-type matrix[6] in a multislice method [7] and includes the effects of absorption [8]. Intensities integrated over all orientations are obtained by summing the results of repeated calculations and the values for a succession of slab thicknesses stored. These infinite-slab results are converted to those for spherical particles by taking appropriately weighted averages. An example is shown in Fig. 4, normalized to the (311) reflection. If the scattering were kinematical the curves would all be horizontal from their values at $D_t = 0$. Variations from (311) (also varying) by a factor of 2 to 3 can be seen at large D_t.

The corrected peak-height data obtained from the plates are used as input to the computer program which performs a simple search procedure to find the best-fitting value of the root mean square amplitude of thermal motion, $\bar{U}$. At every search step the best-fitting scale factor, k, and cluster diameter, D_t, are also found. The function minimized is:

$$R_M = \left[\Sigma(I_{obs} - kI_{calc})^2/\sigma_{obs}^2\right]^{\frac{1}{2}} / \left[\Sigma(I_{obs}/\sigma_{obs})^2\right]^{\frac{1}{2}}$$

The resulting values of D_t, $\bar{U}$, and R_M are reported in Table II. The R_K values are calculated as for R_M, but with "kinematic" I_{calc} and the same $\bar{U}$. In every case R_M is seen to be an improvement over R_K but they are still a good deal larger than the quality of the data would lead us to expect. In addition, if this model and calculation are to be deemed successful, strong correlations between several of the quantities in Table II should be seen. For example, at a given cluster size, $\bar{U}$, and the cell dimension, a, should increase together (indicating higher temperature clusters) and D_t and D_e should agree. A strong indication of the reason for this failure to agree is seen in Figure 5 which shows worsening agreement between observed and calculated intensities with decreasing cluster size. This indicates that the bulk fcc structure is not maintained at small cluster sizes. Further support for this view is found in the consistent pattern of deviations displayed in Figure 6. The most prominent features, (111) observed too strong and (400) too weak, have also been reported for clusters of lead[5] and of argon.[9]

A variety of models, other than the bulk fcc structure, have been considered but all have one or more qualitative features that do not fit the observations. These include the combined fcc plus liquid model[5], stacking faults and twinning between fcc regions, decahedral (pentagonal bipyramid) and icosahedral sphere packing models[10], and a "liquid-like" distribution of vacancies in an fcc matrix. It is reasonable to suppose that a partially liquid or amorphous or "polytetrahedral" structure is correct, but this has not been demonstrated. Single-phase (homogeneous) models other than fcc can be tested with the multi-beam computer program by replacing one subroutine.

ACKNOWLEDGMENTS

We are pleased to thank Mr. K. C. Owen for some oven operating measurements used in Table II, and the Chemistry and Power Branches of the U.S. Office of Naval Research, and the National Science Foundation for partial financial support.

REFERENCES

1) A. Yokozeki and G.D. Stein, J. Appl. Phys., 49, 2224 (1978).

2) C.G. Grangvist and R.A. Buhrman, J. Appl. Phys., 17, 2200 (1976).

3) N. Wada, Jpn. J. Appl. Phys., 6, 553 (1967).

4) H. Blackman, Proc. R. Soc. (London) Ser. A, 173, 68 (1939).

5) A. Yokozeki, J. Chem. Phys., 68, 3766 (1978).

6) L. Sturkey, Acta Crystallogr., 10, 858 (1957). L. Sturkey, Proc. Phys. Soc., 80, 321 (1962). L. Sturkey, Trans. Amer. Cryst. Assoc., 13, 1 (1977).

7) J.M. Cowley and A.F. Moodie, Acta Crystallogr., 10, 609 (1957). P. Goodman and A.F. Moodie, Acta Crystallogr. A, 30, 280 (1974). J.M. Cowley, Diffraction Physics, ch. 10 and 11, esp. section 11.4, p. 234 (New York: American Elsevier, 1975).

8) C.J. Humphries and P.B. Hirsch, Phil. Mag., 18, 115 (1968).

9) J. Farges, B. Raoult, and G. Torchet, J. Chem. Phys., 59, 3454 (1973).

10) C.Y. Yang, J. Cryst. Growth, 47 (1979) 274. K. Heinemann, M.C. Yacaman, C.Y. Yang and H. Poppa, J. Cryst. Growth, 47, 177 (1979).

TABLE I

Oven Operating Pressures a)

Gas	Inlet P_∞ torr b)	P_o/P_∞	Oven P_o torr	P_1/P_o	First Pumping Chamber P_1 torr c)	P_2/P_1	Second Pumping Chamber P_2 torr d) e)
He	2.99	0.10	0.30	0.53	0.16	$< 5\times10^{-5}$	$< 1.6\times10^{-5}$
Ne	7.22	0.14	1.01	0.36	0.36	$< 5\times10^{-5}$	
Ne	9.92	0.16	1.56	0.32	0.51	$< 5\times10^{-5}$	
Ar	3.07	0.14	0.44	0.40	0.18	$< 5\times10^{-5}$	
Ar	5.62	0.18	1.03	0.30	0.31	$< 5\times10^{-5}$	
CO_2	2.88	0.17	0.49	0.38	0.19	$< 5\times10^{-5}$	

a) Gas supply at room temperature (22°C) and oven power off.

b) Measured at inlet of supply tube 10 cm long and 1.5 mm inside diameter.

c) The opening or nozzle between the oven and the first pumping chamber is 0.81 mm in diameter.

d) The opening between the first and second pumping chambers has a diameter of 0.51 mm with a separation between nozzles of 4.3 mm (see Ref. 1 for additional details).

e) Measured over the 15 cm baffle and diffusion pump.

TABLE II

SUMMARY OF EXPERIMENTS AND THEORETICAL COMPARISONS
(Silver Clusters in Various Carrier Gases)

Experiment and Plate No.	Oven Conditions: Carrier Gas	P_o torr	T_o K	Watts	T_{om} K a)	Diffraction Information: a Å	D_e Å b)	D_t Å c)	$\overline{u^2}$ Å d)	R_{fe} e)	R_{fk} f)
6	He	1.28	625	55	1500	4.078	43	37	0.13(5)	10.2	18.0
7		1.28	625	55	1500	4.079	56	-	--	--	--
13		2.90	530	100	1300	4.058	56	37	0.08(12)	14.9	22.3
14		2.90	530	100	1300	4.059	60	50	0.09(4)	15.2	24.7
15		2.90	530	100	1300	4.066	74	-	--	--	--
16*		3.2	545	140	1500	4.066	53	42	0.18(3)	16.6	24.2
8	Ar	0.51	770	50	1300	4.085	72	-	--	--	--
9		0.51	770	50		4.089	72	-	--	--	--
10		0.60	760	45		4.085	68	-	--	--	--
3		1.54	695	50		4.095	69	7	0.15(2)	6.2	9.3
4		1.54	695	50		4.091	69	280	0.14(2)	8.7	17.4
38	CO_2	0.27	625	~30	1100	4.080	46	-	--	--	--
39		0.27	625	1	1100	4.063	50	10	0.17(4)	18.1	21.9
40		0.31	620		1500	4.091	60	-	--	--	--
30*		0.55	720		not observed	4.090	30	60	0.15(6)	32.0	39.0
33	SF_6	0.36	620	~30	1100	4.075	66	180	0.10(7)	11.0	21.6
34		0.36	620	30	1100	4.072	57	-	--	--	--
35		0.37	600	25	1300	4.076	63	-	--	--	--
36		0.37	600	25	1300	4.084	82	-	--	--	--
21		0.37	625	30	1200	4.059	80	260	0.19(2)	11.8	49.9
22*		0.73	625	30	1200	4.065	110	100	0.10(3)	8.7	21.4

a) During an experiment the oven was observed by eye and temperatures judged by filament color.
viz : Red-Yellow ≅ 1100, Yellow ≅ 1200, Yellow-White ≅ 1300, and White ≅ 1500 K.

b) Diameter D_e is from experimentally measured ring widths.

c) Diameter D_t is from theoretical best fit to multislice calculations.

d) Root mean square amplitude of vibration is from multislice calculations with error ± in parenthesis.

e) Agreement parameter from the best fit multislice calculation of peak intensities.

f) Agreement parameter from the theoretical kinematic calculation of peak intensities.

FIGURES

Fig. 1. Schematic diagram of the metal cluster generator with TC - thermocouple, W - prism mirror window, H - heater for metal vaporization, S_1 and S_2 - sets of screws for configuration adjustments, CG-carrier gas, N_1 and N_2 - flow orifices or nozzles.

Fig. 2. Microdensitometer tracings of Experiments 16, 72 and 30 (see Table II). O.D. is the optical density, $\log_{10}(I/I_o)$ and $S = 4\pi\lambda^{-1}\sin(\theta/2)$. Plate 30 is displaced 0.5 O.D. for clarity and Miller indices are shown.

Fig. 3. Experimental cluster size D_e, as a function of oven pressure and temperature determined using Eq. (2) for several metals and carrier gases.

Fig. 4. Theoretical diffracted intensities for fcc silver clusters, normalized to the $\beta(311)$ peak and plotted as a function of diameter D_t.

Fig. 5. The goodness of fit R_M worsens as size D_e decreases, indicating greater deviation from the fcc structure model. Points are labled with the experiment numbers of Table II.

Fig. 6. A detailed comparison, peak by peak, of the observed and calculated Intensities plotted vs. S^2 with Miller indices indicated (see Figs. 2, 5 and Table II).

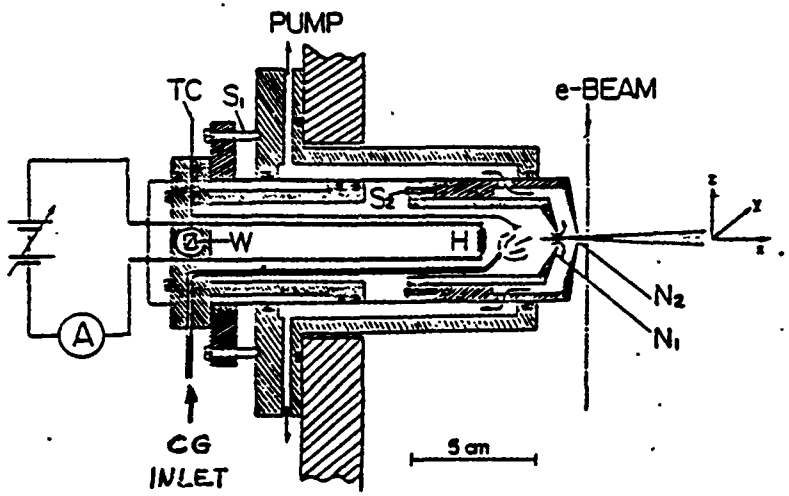

Figure 1

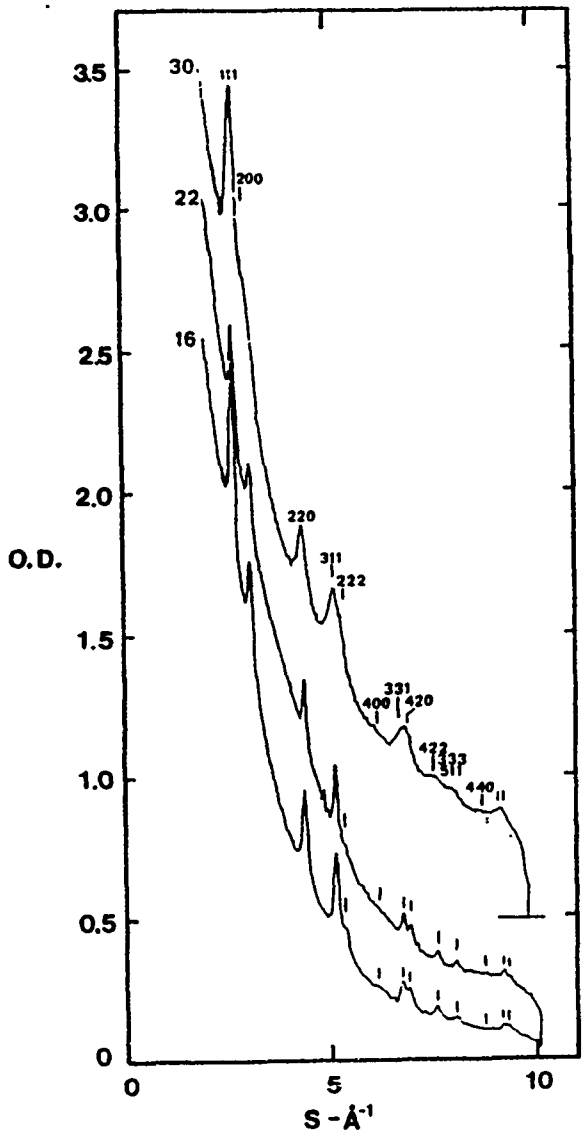

Figure 2

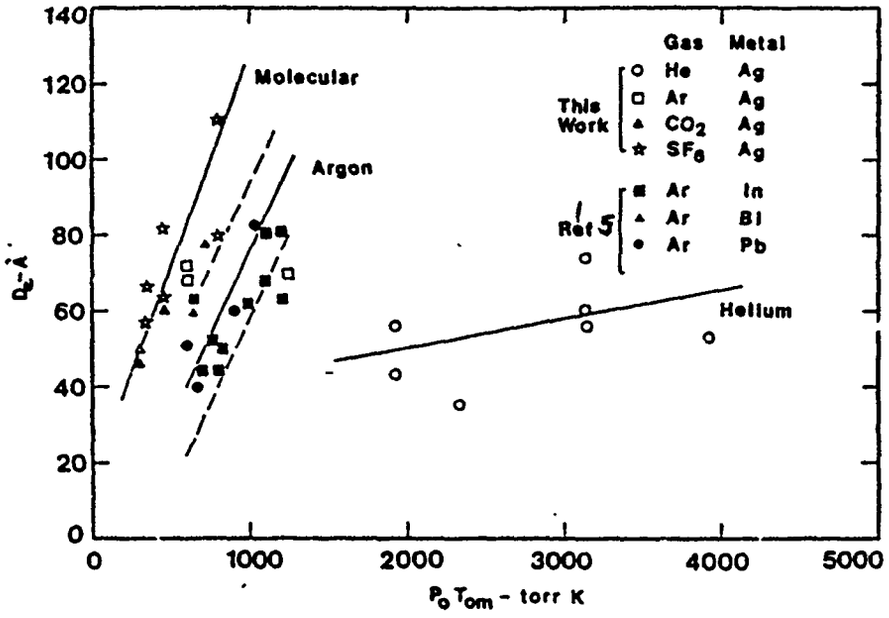

Figure 3

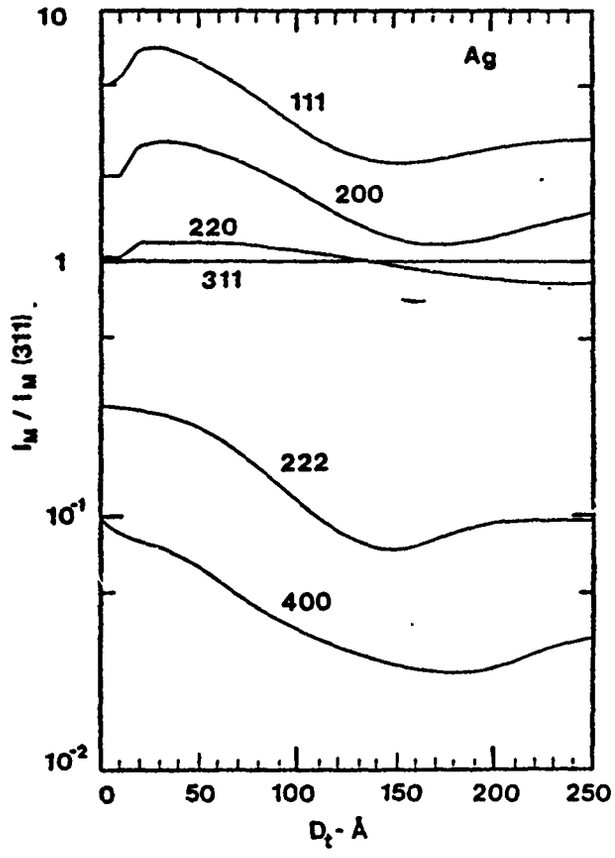

Figure 4

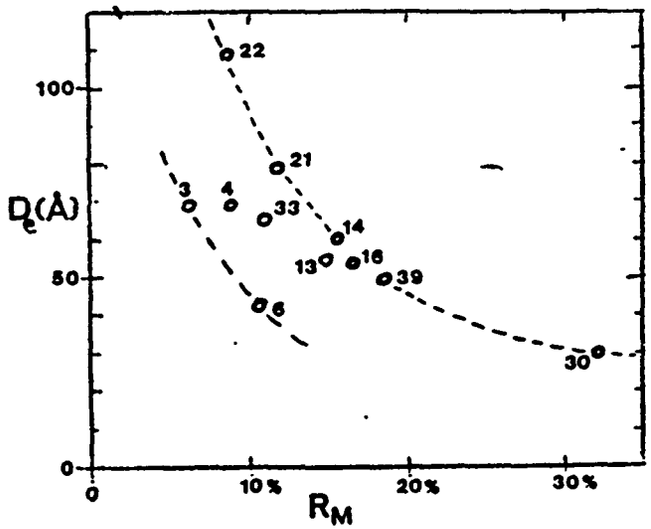

Figure 5

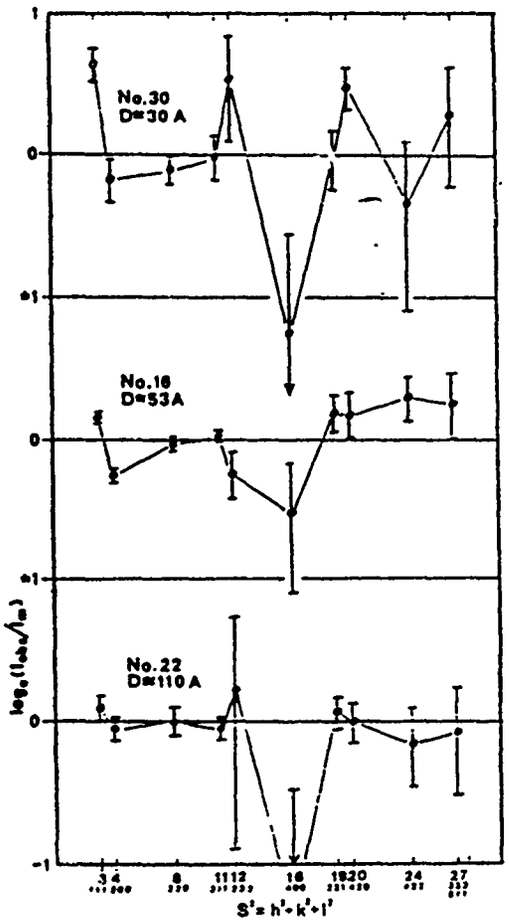

Figure 6